Analysis of CC2 Rigid Pavement Test Data from the FAA's National Airport Pavement Test Facility

D. R. Brill & G. F. Hayhoe
Federal Aviation Administration, Airport Technology R&D Branch, William J. Hughes Technical Center, Atlantic City, New Jersey, USA

L. Ricalde
Galaxy Scientific Corporation, Egg Harbor Township, New Jersey, USA

ABSTRACT: The Federal Aviation Administration (FAA) conducted full-scale traffic tests on new rigid pavement test items at the National Airport Pavement Test Facility (NAPTF). Construction Cycle 2 (CC2) consisted of three independent rigid test pavements on medium-strength subgrade, as well as a smaller test strip constructed on low-strength subgrade. Trafficking of the three CC2 test items began in April 2004 and was completed in December 2004. Tests were conducted using four- and six-wheel simulated aircraft gear loads, and were designed to compare three different support systems: conventional (aggregate) subbase, stabilized (econocrete) subbase, and slab-on-grade. This series of tests yielded significant data on the performance of rigid pavements constructed to current airport standards. This paper summarizes the trafficking data obtained from CC2 tests, and presents an analysis of the relation between gear coverages and pavement performance, making use of the structural condition index (SCI) concept. The performance of the test items is compared to the rigid pavement deterioration model used in FAA's LEDFAA design procedure. Preliminary design factors (DF) for all tests were evaluated using a three-dimensional finite element response model as implemented in the FAA's beta design computer program (FEDFAA). The results of these full-scale tests, supplemented by available data from historical full-scale tests conducted by the U.S. Army Corps of Engineers (COE), will be incorporated into the updated performance/failure models in the FAA's new design procedures for rigid pavements, planned for 2006.

KEY WORDS: Rigid pavement, National Airport Pavement Test Facility, LEDFAA.

1 BACKGROUND AND OBJECTIVES

The National Airport Pavement Test Facility (NAPTF), located at the Federal Aviation Administration (FAA) William J. Hughes Technical Center near Atlantic City, New Jersey, USA, is a unique fully enclosed facility dedicated to full-scale traffic testing of airport pavements under realistic aircraft loads. The facility was built as a cooperative venture of the FAA and the Boeing Company, and was opened in April 1999. Among the goals of the NAPTF testing program is to provide high-quality, full-scale performance and failure data for incorporation into new FAA pavement thickness design procedures, which are planned for completion in 2006.

To date, testing at the NAPTF has consisted of three construction cycles, which were designated CC1, CC2, and CC3. A construction cycle is defined as the complete cycle of planning, construction, trafficking, post-traffic testing and demolition needed to obtain a set of usable data. CC1 was the initial pavement construction consisting of nine pavement test items (six flexible and three rigid), constructed on three different subgrade materials: low strength (target CBR 3-4), medium strength (target CBR 6-7), and high-strength (target CBR 20). Testing of CC1 was completed in November 2001 and the original pavements were subsequently removed. CC2 consisted of three new rigid pavement test items constructed over the medium-strength subgrade, as well as a smaller-scale test strip and test slab. CC3 consisted of four new flexible pavement test items constructed over the low-strength subgrade. The discussion in this paper is limited to the CC2 rigid pavement test items, including the test strip.

The primary objectives of the CC2 tests were: (a) to compare rigid pavement life and performance for different support conditions; (b) to compare pavement life and performance for 4-wheel and 6-wheel gear traffic; and (c) to obtain data on pavement performance as measured by the Structural Condition Index (SCI) versus traffic repetitions. Other objectives included comparing interior and edge stresses under gear loads, and measuring shrinkage and curling of the concrete slabs. To accomplish the first objective, the three CC2 test items were designed with differing foundation types. A three-letter designation is used for each test item. The first two letters refer to the subgrade strength (medium – M) and the surface type (rigid – R), and the last letter refers to the type of construction: C for conventional (aggregate subbase), G for slab placed directly on grade, and S for stabilized (econocrete) base. The structural design information is given in Table 1.

Table 1: Structural Design Data for CC2 Test Items.

Test Item	MRC	MRG	MRS
PCC Surface	30.5 cm (12 in.) PCC (P-501)	30.5 cm (12 in.) PCC (P-501)	30.5 cm (12 in.) PCC (P-501)
Subbase 1	25.4 cm (10 in.) aggreg. subbase (P-154)	none	15.2 cm (6 in.) econocrete base (P-306)
Subbase 2	none	none	21.9 cm (8.6 in.) aggregate subbase (P-154)
Subgrade	Clay (CH) k=35.3 MPa/m (130 pci)	Clay (CH) k=38.0 MPa/m (140 pci)	Clay (CH) k=38.0 MPa/m (140 pci)

The test item layout is shown in Figure 1. All slabs were 4.57 x 4.57 m (15 x 15 ft.). Each of the test items consisted of 20 slabs arranged in four lanes of five slabs, for a total area of 418 m^2 (4,500 ft^2). Test items were separated by paved transition areas 7.6 m (25 ft.) in length. The northern two lanes of slabs were trafficked by carriage 1, while the southern two lanes were trafficked by carriage 2. The basic wander pattern consisted of 33 discrete positions centered on the outside edge of the inside slab (see Figure 1), approximating a normal traffic distribution. While the original plan called for all three test items to be trafficked by 6-wheel traffic on the north side and 4-wheel traffic on the south side, this was actually done only for test items MRG and MRS. For test item MRC, both lanes were trafficked by 4-wheel gears, the difference being that the south side was trafficked by a full wander pattern (i.e., traffic on both the inside and outside slabs), while on the north side a truncated wander pattern was used (traffic applied to the inside lanes only). The gear dimensions are shown in Figure 2.

In general, paving materials were selected to conform to FAA construction standards as set forth in Advisory Circular (AC) 150/5370-10A (FAA, 1999). One significant deviation was the use of a concrete mix with 50% class C fly ash replacing cement. The relatively high replacement rate was intended to reduce the early strength of the mix, thus allowing somewhat thicker slabs that were more representative of airport pavements. It was also felt that thicker slabs would be less likely to exhibit upward curl. Likewise, joints were doweled in both directions, which both enforces uniformity of load transfer at joints and tends to reduce surface stresses in curled slabs. To minimize curling due to differential moisture-related shrinkage, the slabs were hand-watered at periodic intervals from the end of curling through end of traffic testing. Slab corner measurements made during the course of the test using deflection transducers verified that the slabs remained essentially flat. A fuller discussion of the CC2 test strip and test slab experiments that preceded construction of the test items and informed the above design decisions is given in Hayhoe (2004).

Traffic on test item MRC began on April 27 and ended on June 24, 2004. Traffic on test items MRG and MRS began on July 6 and ended on December 10, 2004. The nominal load for all tests was 24,950 kg (55,000 lbs.) per wheel at 1448 kPa (210 psi) tire pressure. A summary of the traffic applied to each test item is presented in Table 2.

Table 2: Traffic Summary for CC2 Test Items.

		Passes Completed			
Test Item	Gear Type	Apr-Jun 2004	Jul-Sep 2004	Oct-Dec 2004	Total
MRC - North	4-wheel	12675	0	0	12675
MRC - South	4-wheel	5405	0	0	5405
MRG - North	6-wheel	0	21186	9834	31020
MRG - South	4-wheel	0	21162	9834	30996
MRS - North	6-wheel	0	20262	0	20262
MRS - South	4-wheel	0	21162	9834	30996

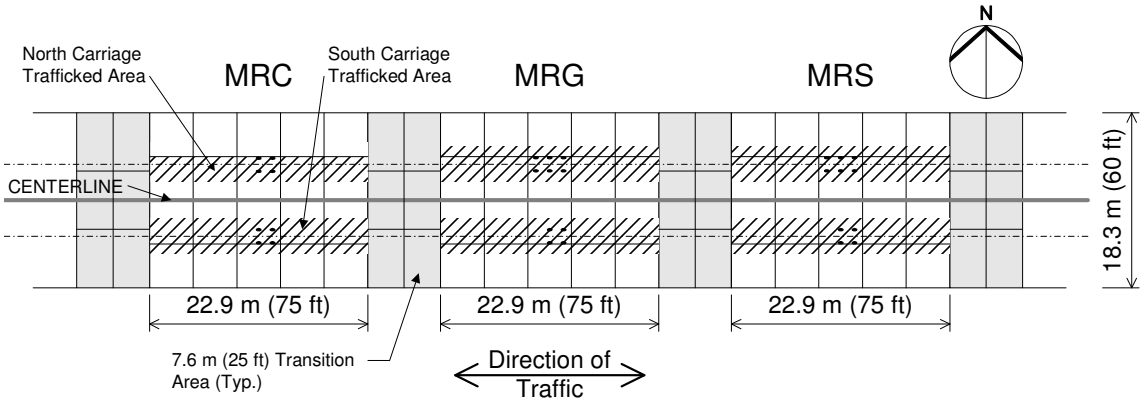

Figure 1: Layout of CC2 test items at the NAPTF.

(a) 6-wheel gear. (b) 4-wheel gear.

Figure 2: Gear load dimensions for CC2 traffic tests.

2 PAVEMENT PERFORMANCE AND DISTRESS MONITORING

Several methods were used to monitor the performance of the CC2 test items during the course of the test:

1. Heavy-weight deflectometer (HWD) tests were conducted prior to testing and at various intervals after the start of testing. These tests were useful in determining at what coverage level the pavement experienced significant loss of bearing capacity.
2. The structural response of the pavement to traffic loading was monitored continuously using embedded sensors. Instrumentation included concrete strain gages, and horizontal and vertical deflection transducers. Anomalous responses from strain gages can indicate the presence of a crack in a concrete slab before it propagates to the surface and becomes visible.
3. Visual surveys of the pavement surface were performed at frequent intervals. Observed distresses were recorded using the procedures in ASTM D 5340-03, "Standard Test Method for Airport Pavement Condition Index Surveys" (ASTM, 2003). From the observed data, a set of detailed distress maps of each test item was prepared showing the progress of the deterioration with additional traffic coverages (Figure 3).

The distress surveys were particularly important for relating the applied coverages to the observed pavement performance. The rigid pavement failure model incorporated in the FAA's LEDFAA thickness design procedure makes use of the structural condition index (SCI) concept originally proposed by Rollings (1988). As defined by Rollings, SCI is the structural component of the pavement condition index (PCI). The SCI is determined using the same procedures as the PCI for rigid pavements, except that only the load related distress types are considered. As a result, the SCI is always equal to or higher than the PCI for the same pavement feature. The specific distresses included by Rollings in the SCI computation were: corner breaks; linear (longitudinal/transverse/diagonal) cracks; shattered slabs; shrinkage cracks (used in this case to describe load-induced linear cracks that do not extend all the way across the slab); and joint and corner spalls. In the present analysis, the same methodology was used for computing SCI, except that joint and corner spalls were excluded from the list of structural distresses. Although significant spalls were observed on some of the NAPTF test items, it was felt that the spalling was primarily a construction-related rather than a load-related distress, and excluding it from the SCI computation led to better correspondence with previous full-scale test data.

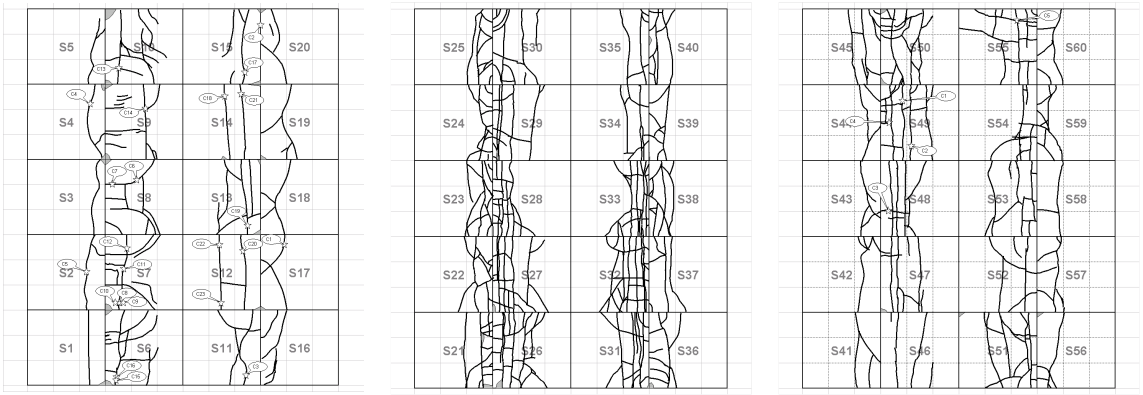

(a) Test Item MRC (b) Test Item MRG (c) Test Item MRC

Figure 3: Final distress maps for CC2 test items. Locations of core samples are indicated by stars. Grayed areas indicate areas where spalling was observed.

It is important to distinguish the SCI as defined by Rollings (1988) and as used in the present analysis from the definition of structural PCI adopted by the U.S. Navy and as implemented in later versions of the MicroPAVER pavement management software (U.S. Army Corps of Engineers CERL, 2004). The latter includes several additional distress types not considered in the original definition and is therefore not consistent with the SCI-based FAA rigid pavement design procedures.

3 ANALYSIS OF SCI VERSUS COVERAGES

In the analysis of the CC2 traffic tests, the change in SCI was taken as the principal measure of pavement performance. The rigid pavement failure model in the LEDFAA design procedure assumes that there is a predictable relationship between the number of coverages at a given load level and the amount of structural distress as represented by the SCI.

A newly constructed pavement has an SCI equal to 100. Initially, as traffic is applied, the SCI remains at 100 although pavement life is being consumed. At the appearance of the first structural crack, the SCI drops below 100, and continues to deteriorate with additional coverages until the pavement is completely failed. The number of coverages at which a first structural crack appears (i.e., at which SCI just drops below 100) is designated by C_O. The number of coverages corresponding to SCI = 0 (total failure, characterized by shattered slabs and significant loss of bearing capacity) is designated by C_F. For design purposes, failure of a rigid pavement is defined by SCI = 80. This is the SCI that would be computed for a pavement in which 50 percent of the slabs exhibit some structural cracking. For a conventional rigid pavement (slab on an unbound aggregate base), the number of coverages to the design failure condition SCI = 80 is obtained by linearly interpolating between C_O and C_F on a plot of SCI versus the log of coverages. As shown in Figure 4, the full-scale tests conducted at the NAPTF generally validate this approach and show that a straight-line model of SCI versus log of coverages is a reasonable assumption for design.

In Figure 4, it is important to distinguish the number of coverages from the number of vehicle passes. The pass-to-coverage ratio (*P/C*) relates these two variables and is a function of the gear configuration for the applied wander pattern. For the basic 66-position wander pattern used in the tests, for both the 6-wheel and 4-wheel gear configurations, the computed pass-to-coverage ratio was 4.71. For the truncated wander pattern used on test item MRC-North, a slightly smaller P/C of 3.80 was computed. The trendlines in Figure 4 were computed as a linear best fit to the observed data points. Following Rollings (1988), the trendlines were extended to the SCI = 100 and SCI = 0 lines in order to obtain the values for C_O and C_F respectively. This method allows the C_O and C_F values to be based on analysis of the entire trend of SCI versus coverages, rather than on single observations, which are subject to high variability. The regression data and the computed values of C_O and C_F for each test are reported in Table 3.

3.1 Distress Modes Observed in CC2 Test Items

As stated above, care was taken to ensure that slabs remained substantially flat and uncurled during testing, and these efforts were successful. Measured uplift at all corners remained at 0.38 mm (15 mils) or less. Nevertheless, top-down cracks were not eliminated in either the outside lanes or the inside lanes. In the inside lanes receiving traffic from both wheels of the dual axle, both top-down and bottom-up fatigue cracks were observed. (The direction of the crack was determined from extracted cores where possible - see Figure 5a.) The outside lanes received either no direct traffic (MRC-N) or traffic from only one wheel of the dual,

suggesting that top-down cracks observed in the outside lanes (Figure 5b) were induced in part by loads transferred through the joints via the dowels. The significant differences in cracking modes observed between the inner and outer slabs complicated the SCI evaluation of the test items, because it is ordinarily assumed that the deterioration of slabs (as measured by change in SCI) is correlated to the amount of traffic applied. In general, however, cracks appeared first on slabs located in the outside lanes, even though those slabs received relatively less traffic from the applied wander pattern (Fig. 1). If all 10 slabs in a given test item were included in the SCI sample, then the early appearance of top-down cracks such as Figure 5(b) would tend to distort the SCI-vs.-coverage analysis, leading to inconsistent values of the C_O factor. For this reason, it was decided to include only those slabs receiving traffic from both tires in the dual module (i.e., the five inside slabs) in the SCI sample units for analysis. For purposes of SCI evaluation on the inside slabs, no distinction was made between visible bottom-up and top-down cracks.

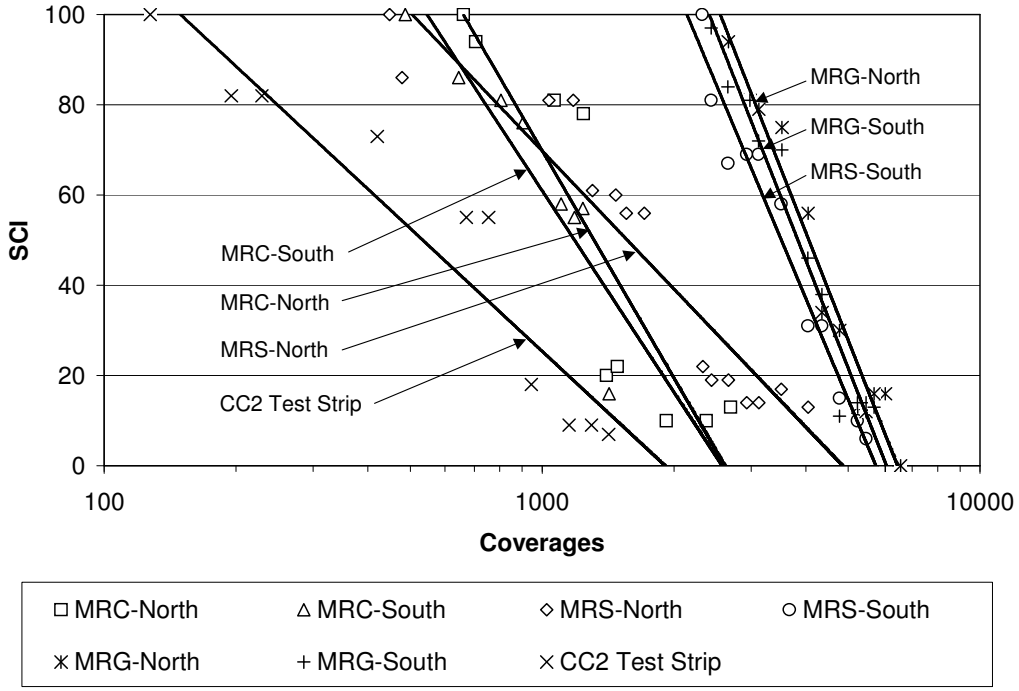

Figure 4: Plot of SCI versus log of coverages for all CC2 test items with trendlines.

Table 3: Regression Data for Analysis of SCI Versus Coverages.

Test Item	Regression Constants[1] A	B	R^2	Coverages to Initial Crack, C_O	Coverages to Full Failure, C_F	P/C
MRC-N	-167.43	572.15	0.821	661	2613	3.80
MRC-S	-148.36	506.04	0.827	546	2576	4.71
MRG-N	-247.03	941.57	0.964	2551	6480	4.71
MRG-S	-246.96	935.12	0.965	2408	6117	4.71
MRS-N	-101.71	374.94	0.896	505	4855	4.71
MRS-S	-231.66	871.57	0.961	2141	5784	4.71
Test Strip	-90.33	296.37	0.904	149	1910	4.13

[1] $\mathrm{SCI} = A \log(C) + B$

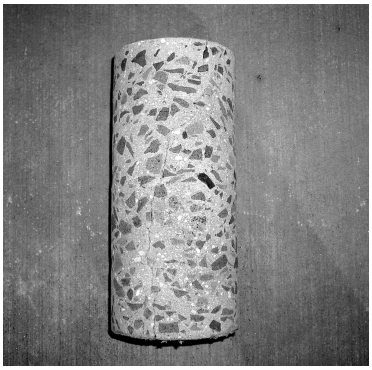

(a) Core sample showing a bottom-up crack in test item MRS-South

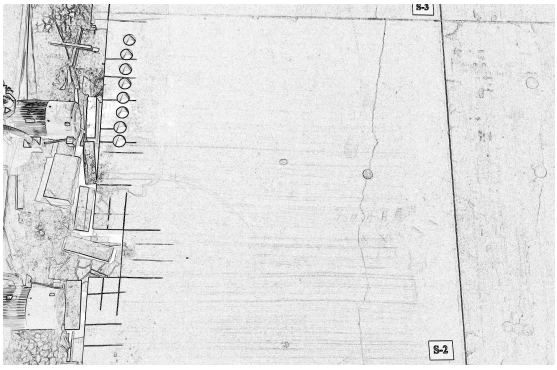

(b) Top-down crack observed in outside lane of test item MRC-North (Slab S-2)

Figure 5: Examples of fatigue cracks observed in CC2 test items.

3.2 CC2 Test Strip Results

Figure 4 and Table 3 contain data for the CC2 Test Strip in addition to the main CC2 test items described above. These results were obtained from the full-scale trafficking to failure of the test strip conducted in March-April 2002. The test strip layout is illustrated in Figure 6. Traffic, consisting of a dual-tandem gear with 24,950 kg (55,000 lbs.) per wheel, was applied to the shaded area in Figure 6. The gear configuration was similar to Figure 2(b), except that the dual spacing was 111.8 cm (44 in.). There were other significant differences between the test strip construction and the other CC2 test items that could have impacted its performance to a unknown degree:

- The test strip was constructed over a low-strength silty clay (CBR 4-5), rather than the medium strength clay (CBR 7-8) used for the other test items. The structure above the subgrade consisted of a 27.9 cm (11 in.) slab, supported by a 15.6 cm (6.1 in.) econocrete stabilized base, on a 21.3 cm (8.4 in) aggregate subbase layer.
- The test strip slabs were doweled in the longitudinal direction only. Transverse joints were weakened-plane contraction joints. Since there were only two lanes, the outside edges were effectively free.
- No fly ash was used in the test strip concrete mix. Hence, the effective flexural strength of the concrete slabs was higher than for the other CC2 test items.
- Curing procedures varied from slab to slab. This was part of the experiment that established the test procedures for the main CC2 test items.

As shown in Figure 6, there were two sizes of test strip slabs built, 6.1 x 6.1 m (20 x 20 ft.), and 4.6 x 4.6 m (15 x 15 ft.). Because significant upward curl leading to premature load-induced corner breaks was observed on the four 6.1 m (20 ft.) slabs, these slabs were excluded from the performance analysis. The two lanes of slabs designated “S Slabs” and “C Slabs” were distinguished by the concrete mix used. As discussed in McQueen *et al*. (2002), the S slabs used a three-part “optimized” aggregate mix, while the C slabs used a two-part aggregate mix similar to the original CC1 experiment. Consistent with the analysis of the other CC2 test items, only the slabs receiving traffic from both wheels of the dual module (i.e., the S slabs) were included in the SCI calculation. Hence, the SCI values reported in Figure 4 for the test strip are based on four of the twelve slabs (the 4.6 m S slabs only). Design factors, discussed below, were computed for the test strip based on the S slab properties.

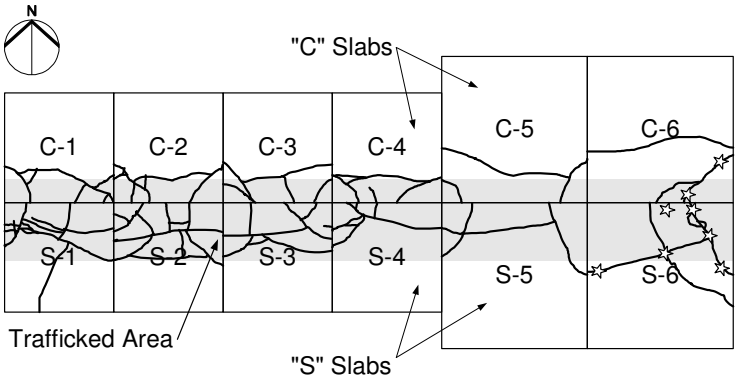

Figure 6: Final distress map for CC2 test strip.

3.3 Stabilized and Non-Stabilized Test Items

The CC2 traffic tests enabled a direct three-way comparison of conventional (aggregate base), stabilized base, and slab-on-grade construction. It is generally believed that one of the benefits of stabilized bases for rigid pavements, which are required by the FAA for airports accepting aircraft of over 45,360 kg (100,000 lbs.), is that they provide additional pavement durability beyond the initial cracking phase. The LEDFAA pavement design procedure accounts for this benefit by extending the downward leg of the SCI-vs.-coverages curve as shown in Figure 7. Figure 7 compares the data points from test items MRS-N and MRS-S with the current LEDFAA rigid pavement failure model (FAA 2004) including stabilized base compensation. It is clear from the curves in Figure 7 that the nonlinear trend in the current LEDFAA failure model does not represent the actual post-cracking behavior of a stabilized base structure under traffic. Rather, the data indicate that, regardless of whether or not a stabilized base is used, the deterioration of the SCI is best represented by a model that is linear in the log of coverages.

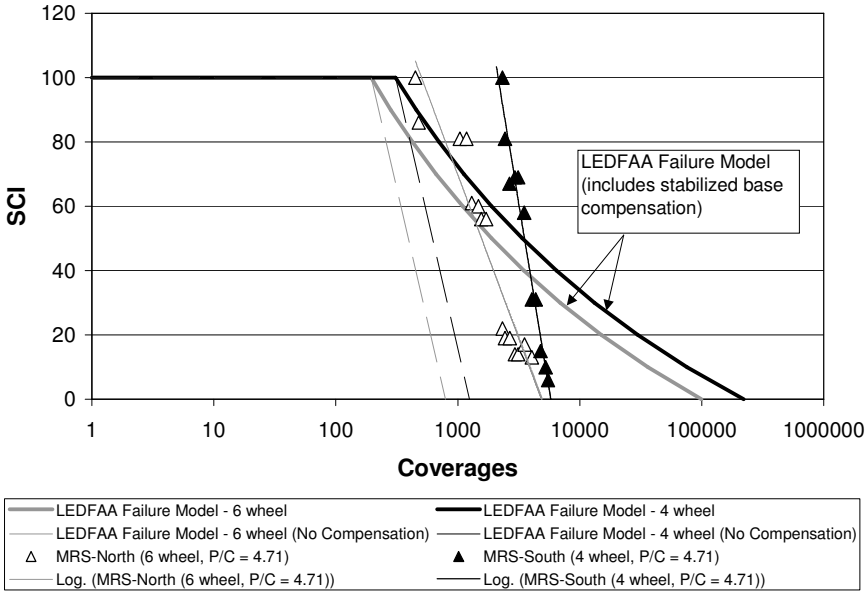

Figure 7: SCI vs. coverage curves for stabilized base test items, comparing observed data points with the current LEDFAA rigid pavement failure model.

In general, the results of the CC2 tests support the principle that higher quality subbases extend the useful life of the pavement, and this extra durability is reflected in the slope of the SCI-vs.-log(C) trendline. Examining Figure 4, it is seen that the two test items producing markedly flatter slopes (MRS-N and Test Strip) are both stabilized base structures, while in Table 3 it is shown that the slope of the trendline (parameter *A*) is generally highest for stabilized structures, somewhat steeper for the conventional structures (MRC), and highest for the slab placed directly on the subgrade soil (MRG). Indeed, it was observed that the MRG test items progressed rapidly to complete failure once cracking initiated. The only exception to the general rule was test item MRS-S, which exhibited a slope more consistent with the MRG structures. The reason for this exception is being further investigated.

As seen in Figure 7, the compensation for high-stiffness bases in LEDFAA can be significant and results in reduced design thicknesses for both new pavements and overlays on stabilized subbases. The degree of deviation from the basic straight-line relationship (the dashed line in Fig. 7) is of critical importance for rigid overlay designs, which are concerned with the lower portion of the curve for SCI between 40 and 80. For new rigid pavement designs, where the thickness is determined by the intersection of the curve with the SCI 80 line, stabilized base compensation is less critical but still significant. For the FAA rigid design procedures now under development, calibration studies are being performed comparing both stabilized base and conventional thickness designs to the current FAA standard in AC 150/5320-6D (FAA 2004). These comparisons will be used to determine the appropriate modification to the basic rigid pavement failure model for stabilized bases.

4 ANALYSIS OF DESIGN FACTOR VERSUS COVERAGES

The LEDFAA rigid pavement failure model is based on an analysis of several previous full-scale traffic tests conducted by the U.S. Army Corps of Engineers (COE) between 1943 and 1974 (Parker *et al.* 1979). Rollings (1988) obtained the following regression equations:

$$DF = 0.5234 + 0.3920 \log(C_O) \quad (1a)$$

$$DF = 0.2967 + 0.3881 \log(C_F) \quad (1b)$$

where *DF*, the design factor, is the ratio of the concrete flexural strength to the computed design stress. For a given *DF*, linear interpolation between C_O and C_F on the SCI-vs.-log(*C*) plot yields the dashed lines shown in Figure 7. The regression constants were derived from analysis of 30 data points with *DF*s computed using layered elastic analysis of the test sections. The FAA's new pavement thickness design program FAARFIELD, planned for completion in 2006, will update equations 1(a) and (b) by deriving new regression constants based on:

- Re-analysis of the original full-scale test data with design factors computed using three-dimensional finite element (3D-FE) edge stresses in lieu of layered elastic (interior stresses). This will make the failure model consistent with the rigid pavement structural model that will be used to obtain design stresses in FAARFIELD.
- Inclusion of seven new data points from the CC2 tests (MRC-North and -South, MRG-North and -South, MRS-North and -South, and the test strip).

To date, preliminary design factors based on the 3D-FE structural model as implemented in the FAA's beta design program FEDFAA (http://www.airporttech.tc.faa.gov) have been computed for both CC2 and historical full-scale tests using available information for COE tests (Parker *et al.* 1979, Rollings 1988). The CC2 design factors will be finalized in the near future based on material characterization test results from post-traffic testing at the NAPTF.

5 CONCLUSIONS

Rigid pavement full-scale traffic tests recently completed at the FAA's National Airport Pavement Test Facility provided pavement performance and failure data for three new rigid pavement test items and a test strip. The performance data were analyzed using the SCI concept to obtain coverages to initiation of structural cracking and to full structural failure. Test results are being analyzed currently in conjunction with previous full-scale tests and will be used to update the failure model for rigid pavement and overlay design in future FAA design software.

ACKNOWLEDGMENTS/DISCLAIMER

The work described in this paper was supported by the FAA Airport Technology Research and Development Branch, Dr. Satish K. Agrawal, Manager. The contents of the paper reflect the views of the authors, who are responsible for the facts and accuracy of the data presented within. The contents do not necessarily reflect the official views and policies of the FAA. The paper does not constitute a standard, specification, or regulation.

REFERENCES

American Society for Testing and Materials (ASTM), 2003. *Standard Test Method for Airport Pavement Condition Index Surveys*. Designation D 5340-03, ASTM International, West Conshohocken, Pennsylvania, USA.

Federal Aviation Administration (FAA), 1999. *Standards for Specifying Construction of Airports*. Advisory Circular (AC) 150/5370-10A, FAA, Washington, DC.

Federal Aviation Administration (FAA), 2004. *Airport Pavement Design and Evaluation*. Advisory Circular (AC) 150/5320-6D, Change 3, FAA, Washington, DC.

Hayhoe, G.F., 2004. "Traffic Testing Results from the FAA's National Airport Pavement Test Facility," *Proceedings of the 2nd International Conference on Accelerated Pavement Testing*, University of Minnesota, Minneapolis, Minnesota, USA.

McQueen, R.D., Rapol, J., and Flynn, R., 2002. "Development of Material Requirements for Portland Cement Concrete Pavements at the FAA National Airport Pavement Test Facility." *Proceedings of the 2002 FAA Worldwide Airport Technology Transfer Conference*, Atlantic City, New Jersey, USA.

Parker, F., Barker, W.R., Gunkel, R.C., and Odom, E.C., 1979. *Development of a Structural Design Procedure for Rigid Airport Pavements*. Report FAA-RD-77-81, Federal Aviation Administration, Systems Research and Development Service, Washington, DC.

Rollings, R.S., 1988. *Design of Overlays for Rigid Airport Pavements*. Report No. DOT/FAA/PM-87/19, Federal Aviation Administration, Washington, DC.

U.S. Army Corps of Engineers Construction Engineering Research Center (CERL), 2004. *Micro PAVER 5.2 Users Manual*. M.Y. Shahin, Principal Investigator, U.S. Army Corps of Engineers ERDC-CERL, Champaign, Illinois, USA.